KOREAN JOURNAL OF PACKAGING SCIENCE & TECHNOLOGY
Vol. 32, No. 2 117~123 (2026)
https://doi.org/10.20909/kopast.2026.32.2.117

COMSOL-Based Placement Design of Printed Piezoelectric Sensor Labels for Shock Monitoring in Transport Packaging

Omkar Y. Pawar[1], Siyoung Yang[2]* and Sooman Lim[1]*

[1]*Graduate School of Flexible and Printable Electronics, LANL-JBNU Engineering Institute-Korea, Jeonbuk National University, Jeonju 54896, Republic of Korea*

[2]*Department of Mineral Resources and Energy Engineering, Research Institute of Energy and Mineral Resources Development, Jeonbuk National University, Jeonju 54896, Republic of Korea*

Abstract Printed piezoelectric sensor labels can convert package deformation into electrical signals, but their response depends strongly on where the label is attached to the package surface. In this study, a static-equivalent top-impact placement-screening method was constructed for printed PVDF/carbon nitride nanotube (CNNT) piezoelectric sensor labels on a corrugated transport package. A 200 mm × 120 mm × 100 mm package model was used, and four label regions were compared: central-edge, adjacent, side, and impact-reference positions, using the domain-averaged von Mises stress. The directly impacted label served only as a normalization reference, and results were reported as stress-transfer factors and reference-normalized voltage-equivalent indices rather than measured dynamic voltages. At 40 N, the central-edge, adjacent, and side positions reached stress-transfer factors of 0.6953, 0.6034, and 0.2434, respectively. These factors identify the central-edge region as the most suitable off-impact placement. The framework provides a reproducible way to screen sensor-label positions before dynamic drop testing and full package validation.

Keywords Printed piezoelectric sensor; PVDF/CNNT; Transport packaging; Static-equivalent analysis; Sensor placement

Introduction

Transport packaging is designed to reduce mechanical damage during stacking, sorting, loading, delivery, and storage.[1-5] In parcel delivery, local impact or compression may occur at only a small region of a package, while the damaged product can remain visually hidden inside the box. This limitation has increased interest in smart packaging systems that can record or indicate handling history. Existing visual indicators and electronic loggers can provide useful information, but they may require separate batteries, bulky modules, or additional attachment processes. Thin printed sensor labels offer a different route because they can be integrated onto the package surface with limited changes to the package form factor.[6]

*Corresponding Author: Siyoung Yang and Sooman Lim
Graduate School of Flexible and Printable Electronics, LANL-JBNU Engineering Institute-Korea, Jeonbuk National University, Jeonju 54896, Republic of Korea
Department of Mineral Resources and Energy Engineering, Research Institute of Energy and Mineral Resources Development, Jeonbuk National University, Jeonju 54896, Republic of Korea
Tel: +82-01-063-270-4259
E-mail: smlim@jbnu.ac.kr (S. Lim); yangsy@jbnu.ac.kr (S. Yang).

Piezoelectric polymer sensors are attractive for such sensor-label concepts because they can generate an electrical response from mechanical deformation without an external power source.[7,8] Poly(vinylidene fluoride), abbreviated as PVDF, and its composites have been widely studied because their flexible film geometry is compatible with printed, laminated, or label-type devices.[9-13] The piezoelectric response of a PVDF-based label, however, is not determined by d_{33} or beta-phase fraction alone. In package-scale use, the local stress field at the attachment position also controls the mechanical input delivered to the sensor. Therefore, a material with good piezoelectric output can still produce a weak package-level signal if the label is attached to a low-stress region.

For corrugated transport boxes, sensor placement is not straightforward.[14-17] A directly impacted region gives a high signal, but the actual impact point is not known before distribution. A side-wall label may be easy to attach and read, but it may receive only a small portion of top-impact stress. A workable sensor-label design therefore needs a screening method that compares candidate positions using the same package geometry and loading condition. Finite-element analysis is useful for this purpose because it can compare stress transfer at multiple positions before fabrication and drop testing.[18,19] However, finite-element stress should not be directly reported as measured voltage unless the dynamic loading, adhesive transfer, sensor layer thickness, electrode geometry, and time-domain output are validated experimentally.

This study proposes a conservative static-equivalent placement-screening framework for a printed PVDF/carbon nitride nanotube (CNNT) piezoelectric sensor label on a corrugated transport package. The sensor material basis was taken from a previously reported PVDF/CNNT film prepared by direct ink writing,[6] while the package-scale analysis was newly organized around four label positions: central-edge, adjacent, side, and impact-reference domains. The impact-reference domain was not treated as a recommended attachment position; it was used as an internal reference for normalization. The main output of the present work is therefore not a dynamic shock voltage, but a reference-normalized voltage-equivalent index derived from domain-averaged von Mises stress. This framing allows the simulation data to support placement design while avoiding claims that require dynamic drop-test evidence.

Materials and Methods

1. Sensor-material basis and calibration separation

The printed sensor label was defined using a PVDF/CNNT composite film previously reported for piezoelectric energy conversion.[6] In that material system, the CNNT content was used to tune the phase structure and piezoelectric output of PVDF. The 7.5 wt% PVDF/CNNT composition was used as the material basis in the present placement study because it provided a higher d_{33} value than pristine PVDF and a usable flexible-film form for attachment to package surfaces.

The printed sensor labels were fabricated by the direct ink writing process reported for the same PVDF/CNNT system.[6] The CNNT filler was first obtained by thermal polycondensation of a nitrogen-rich precursor, followed by a structural transformation of graphitic carbon nitride from a two-dimensional sheet architecture to a one-dimensional nanotube architecture. A printable composite ink was then prepared by dissolving PVDF in N,N-dimethylformamide and dispersing the CNNT filler at 7.5 wt% under stirring and sonication until a homogeneous ink was obtained. The ink was extruded through a fine nozzle and deposited layer by layer onto the substrate by direct ink writing, and the shear flow during extrusion promoted beta-phase formation and dipole alignment so that a separate strong poling step was not required. After solvent evaporation and mild drying, electrodes were applied to both faces of the printed film, which was then cut and packaged into a thin flexible label suitable for attachment to a package surface. In the present placement study this fabricated PVDF/CNNT label was used only as the sensor-material basis, while the package-scale response at each candidate position was evaluated with the static-equivalent COMSOL model.

Table 1. Sensor-material information and calibration usage. The published dynamic output and the static-equivalent package-scale index are separated to avoid overinterpretation.

Item	Value	Unit
Pristine PVDF d_{33}	5.2	pC/N
PVDF/CNNT 7.5 wt% d_{33}	18.4	pC/N
PVDF/CNNT 7.5 wt% beta-phase	35.9	%
Published dynamic output under 40 N	ca. 12	V
Reconstructed force-voltage slope	0.2033	V/N
Reconstructed force-voltage intercept	0.2469	V
Fabricated sensor film size	30 × 30	mm
Fabricated sensor film thickness	0.06	mm

The fabricated PVDF/CNNT sensor film used for label preparation had dimensions of 30 mm × 30 mm and a thickness of 0.06 mm. This dimension is reported as the fabricated film size and should be distinguished from the package-scale sensor-domain definition used in the static-equivalent COMSOL model.

The sensor-material values and package-scale indices were separated in this study. The published dynamic output of ca. 12 V under 40 N was retained as a published sensor-material output, but it was not used as the static package-scale voltage. Instead, the present package simulation used the reconstructed force-voltage relationship only to express a voltage-equivalent index after stress normalization. This separation is necessary because the finite-element result in this study is a static-equivalent stress field, whereas the published voltage was obtained from a dynamic sensor test. These sensor-material values and their calibration usage are summarized in Table 1.

2. Package geometry and sensor-position design

A corrugated transport package with external dimensions of 200 mm × 120 mm × 100 mm was used as the model geometry. The package was simplified as an equivalent continuum body in order to focus on package-level stress transfer rather than flute-scale local buckling.[14-17] The top face was loaded through a square impact pad, and four label regions were defined on the package surface. The central-edge label was placed on the top face near the central edge region, the adjacent label was placed on the top face away from the direct impact point, the side label was placed on the side wall, and the impact-reference label was placed under or near the direct loading path.

The impact-reference label was included to define the internal reference level of the package model. This position is expected to receive the highest local mechanical input under top loading, but it is not an ordinary placement candidate because the actual impact point cannot be selected in advance during parcel distribution. The off-impact positions were

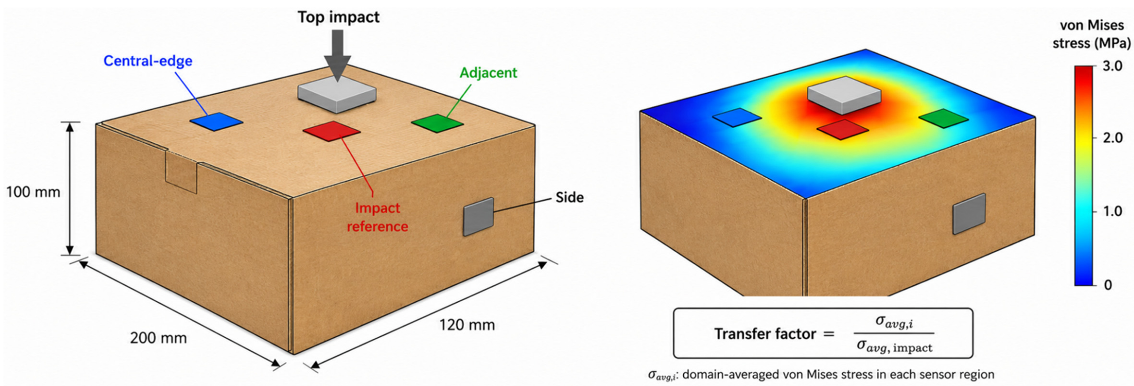

Fig. 1. Static-equivalent top-impact placement-screening framework for printed piezoelectric sensor labels on a 200 mm × 120 mm × 100 mm corrugated transport package. The central-edge, adjacent, side, and impact-reference label domains are compared using the domain-averaged von Mises stress. The impact-reference sensor is used only as a direct-stress reference.

therefore evaluated against the reference position using a stress-transfer factor. Fig. 1 illustrates the package dimensions, label locations, top-impact pad, and normalization concept.

3. Static-equivalent structural model and mesh

The structural model was built as a quasi-static top-impact problem.[18,20] A vertical load was applied to the top impact pad and transferred to the package surface. The lower package support was constrained to prevent rigid-body motion. The label regions were defined as surface or thin-domain regions for extracting local domain-averaged stress. The present model does not include impact duration, acceleration history, rebound, damping, adhesive viscoelasticity, or nonlinear crushing of the corrugated board. These assumptions define the work as a static-equivalent placement-screening study rather than a complete drop-impact prediction.

Mesh refinement was applied around the impact pad and label domains because these regions determine the extracted stress values. The model was used as a structured placement-screening model, not as an isolated point-stress reading. The package dimensions, equivalent wall thickness, impact pad size, package-scale sensor-domain size, boundary condition, load condition, mesh strategy, and extracted quantity are summarized in Table 2. The retained model geometry and mesh distribution are shown in Fig. 2.

4. Domain-averaged stress and voltage-equivalent index

The mechanical response at each sensor position was summarized using the domain-averaged von Mises stress.[18] For the i-th label domain, the average stress was defined as the mean of the von Mises stress over the label region. This approach avoids the sensitivity of a single point value to mesh density or local geometric singularities.

The stress-transfer factor was calculated as the ratio of the domain-averaged stress at a label position to the domain-averaged stress at the impact-reference domain. At a load of 40 N, the effective load index was calculated as this factor multiplied by 40 N. The voltage-equivalent index was then calculated as 0.2033 times the effective load index plus 0.2469. This index should be read as a reference-normalized signal index, not as a measured voltage under package drop impact.

Table 2. Static-equivalent package model information used in the placement study

Model item	Value
Package dimensions	200 mm × 120 mm × 100 mm
Equivalent model representation	Equivalent corrugated-board continuum
Equivalent wall thickness	2 mm
Impact pad	30 mm × 30 mm square top pad; area = 900 mm
Package-scale sensor domain	20 mm × 20 mm × 0.1 mm thin domain; area = 400 mm
Fabricated sensor film/label size	30 mm × 30 mm × 0.06 mm
Sensor domains	Central-edge, adjacent, side, and impact-reference domains
Boundary condition	Lower support constrained to suppress rigid-body motion
Load condition	Static-equivalent top load of 5, 10, 20, 30, 40, and 45 N
Mesh strategy	Refined around the top pad and sensor domains
Main extracted quantity	Domain-averaged von Mises stress

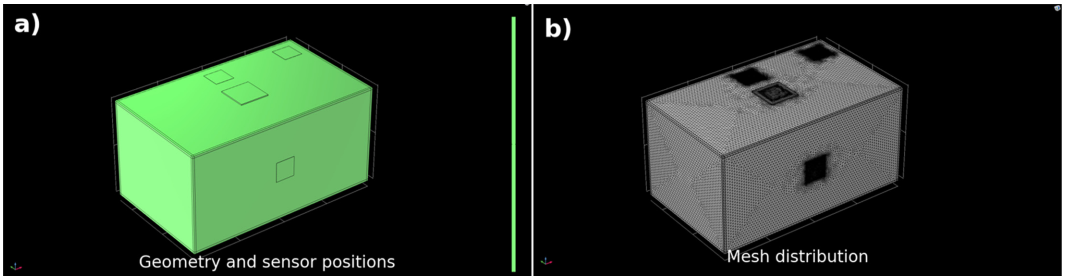

Fig. 2. COMSOL model configuration retained for reproducibility: (a) package geometry and sensor-domain positions, and (b) mesh distribution refined around the label domains and impact region. The image documents the geometry and mesh basis of the static-equivalent placement-screening model.

The index allows different label positions to be compared under one controlled structural model.

Results and Discussion

1. Placement concept and Fig. 1

Fig. 1 presents the placement-screening concept for the printed sensor labels on the transport package. The package dimensions are 200 mm in length, 120 mm in depth, and 100 mm in height, and the figure uses the domain-averaged von Mises stress as its graphical basis, consistent with the data-extraction method applied in the Results section.

The figure-driven layout is intentionally simple. The left panel shows where the four label domains are attached, while the right panel presents the stress-map concept and the reference-normalized transfer factor. This organization separates the physical package geometry from the data-reduction method. It also clarifies that the impact-reference label is not proposed as the main product sensor, but is used as the reference denominator for stress transfer.

2. Load-dependent domain-averaged stress response

The full load-dependent dataset is listed in Table 3 and plotted in Fig. 3. All four sensor regions exhibited nearly proportional increases in domain-averaged von Mises stress as the applied top load increased from 5 N to 45 N. A linear fit to each region in Fig. 3 gave a coefficient of determination of R^2 = 1.0000, confirming that the simulated response remained in a linear range under the present static-equivalent conditions.

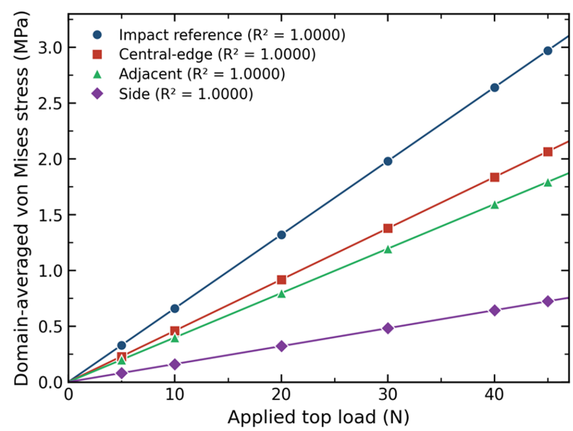

Fig. 3. Load-dependent domain-averaged von Mises stress for the central-edge, adjacent, side, and impact-reference sensor-label regions under static-equivalent top loading. Symbols are the values extracted from Table 3 and the solid lines are linear fits, giving R^2 = 1.0000 for all four regions.

ecause the same package geometry and mesh strategy were used for all label domains, the relative order of the stress response can be compared directly.

The impact-reference label carried the largest stress at every load level. At 40 N, the impact-reference domain reached 2.6407 MPa. Among the off-impact candidates, the central-edge domain recorded the largest value, 1.8362 MPa, followed by the adjacent domain at 1.5934 MPa and the side domain at 0.6428 MPa. The side label therefore received only a small portion of the top-load stress field, which is consistent

Table 3. Full domain-averaged von Mises stress dataset extracted from each sensor-label region

Load (N)	Central-edge (MPa)	Adjacent (MPa)	Side (MPa)	Impact reference (MPa)
5	0.2295	0.1992	0.0804	0.3301
10	0.4591	0.3984	0.1607	0.6602
20	0.9181	0.7967	0.3214	1.3204
30	1.3772	1.1951	0.4821	1.9805
40	1.8362	1.5934	0.6428	2.6407
45	2.0658	1.7926	0.7232	2.9708

with its position away from the loaded top surface.

3. Reference-normalized response at 40 N

The 40 N load condition was selected for direct comparison because it corresponds to the force level used in the reconstructed sensor calibration. Table 4 and Fig. 4 summarize the stress-transfer factor, effective load index, and voltage-equivalent index at this condition. The central-edge sensor had a stress-transfer factor of 0.6953, which corresponds to an effective load index of 27.81 N and a voltage-equivalent index of 5.90 V. The adjacent sensor had a stress-transfer factor of 0.6034, corresponding to 24.14 N and 5.15 V. The side sensor had a much lower transfer factor of 0.2434, corresponding to 9.74 N and 2.23 V.

The impact-reference position produced 8.38 V as a voltage-equivalent index under the same formula. The package-scale index is lower than the published dynamic output of approximately 12 V at 40 N because the two values have different meanings. The 12 V value is a dynamic sensor-material output from the original film test, whereas 8.38 V is a static-

Table 4. Reference-normalized stress transfer and voltage-equivalent index at 40 N. The impact-reference sensor is retained as a reference and is not treated as an ordinary candidate position.

Position	Avg stress at 40 N (MPa)	Transfer factor	Effective load index (N)	Voltage-equivalent index (V)	Role
Central-edge sensor	1.8362	0.6953	27.81	5.90	Best off-impact candidate
Adjacent sensor	1.5934	0.6034	24.14	5.15	Secondary off-impact candidate
Side sensor	0.6428	0.2434	9.74	2.23	Low-response side position
Impact-reference sensor	2.6407	1.0000	40.00	8.38	Direct-stress reference only

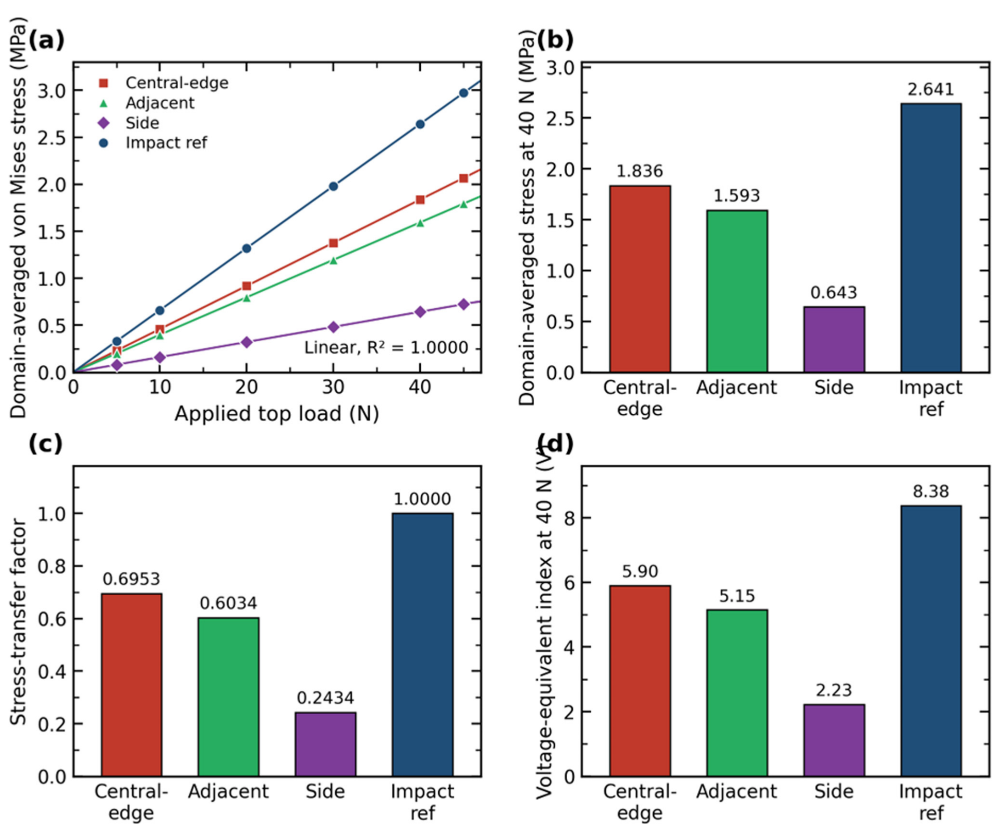

Fig. 4. Domain-averaged sensor-label response under static-equivalent top loading: (a) average von Mises stress versus applied load, (b) average stress at 40 N, (c) stress-transfer factor relative to the impact-reference domain, and (d) voltage-equivalent index calculated from the reconstructed force-voltage relation.

equivalent package-scale index reconstructed through the reference-normalized stress pathway. This study therefore avoids the term predicted voltage and uses voltage-equivalent index to reduce the risk of misinterpretation.

4. Sensor-placement implications for transport packaging

The central-edge position is the most suitable off-impact candidate under the present model. It is not directly under the impact pad, yet it retains about 69.5% of the impact-reference stress at 40 N. This position is useful for label attachment because it balances mechanical sensitivity and practical placement. The adjacent top-surface position also retains a meaningful portion of the stress field, about 60.3% of the reference value, and may be used when the central-edge region is not available because of printing, sealing, barcode, or handling requirements.

By contrast, the side position is less favorable for detecting top-impact events because its stress-transfer factor is only about 24.3% at 40 N. This does not mean that a side-mounted sensor is useless in every distribution environment. Side-wall labels may still be suitable for side compression, lateral impact, or stacking-related deformation. For the specific top-impact scenario analyzed here, however, the side wall is mechanically separated from the main top-surface stress field. A side sensor would therefore require either higher material sensitivity, a different electrode design, or placement closer to a structural edge that carries more load.

The results also explain why a direct impact-reference label should not be interpreted as the recommended sensor position. The directly loaded region gives the largest response, but parcel impacts are spatially uncertain. A real product label must be attached where it can detect likely deformation events without knowing the exact impact point in advance. For this reason, the reference position is used as a normalization standard, and the off-impact positions are evaluated as practical candidates. This interpretation gives the paper a clear design output: central-edge first, adjacent second, and side only for different loading scenarios or secondary monitoring.

5. Scope and limits of the static-equivalent index

The proposed index is intentionally limited. It does not model the time-domain waveform of a package drop, the acceleration history of a transported product, or the voltage generated by a complete sensor circuit.[19,20] It also does not include local crushing of the corrugated flute, adhesive-layer shear lag, electrode resistance, or contact changes between the product and package wall. These factors can change the absolute voltage measured in a dynamic experiment. The voltage-equivalent index should therefore be used only to compare candidate label positions under identical model assumptions.

Even with these limits, the static-equivalent method is useful at the early design stage. Dynamic drop testing of every label position is costly and time-consuming.[18] A finite-element screening map can reduce the test matrix by selecting a smaller number of high-probability positions before sensor fabrication and packaging trials. For packaging research, this approach also connects printed electronics to a practical packaging problem: where a sensor label should be attached on a transport package to obtain a measurable mechanical response.

Conclusions

A static-equivalent top-impact placement-screening framework was prepared for printed PVDF/CNNT piezoelectric sensor labels on a corrugated transport package. The package dimensions were fixed at 200 mm × 120 mm × 100 mm, and four label regions were compared using domain-averaged von Mises stress. Fig. 1 and the retained COMSOL geometry and mesh image document the model geometry and data-extraction basis.

At 40 N, the central-edge, adjacent, and side positions reached stress-transfer factors of 0.6953, 0.6034, and 0.2434 relative to the impact-reference domain. The corresponding voltage-equivalent indices were 5.90, 5.15, and 2.23 V. The central-edge position was therefore selected as the best off-impact candidate for top-impact placement screening, with the adjacent top-surface position as a secondary candidate. The side position gave a lower top-impact response and should be reserved for other loading directions or secondary monitoring functions.

The present index is not a substitute for dynamic drop-test voltage measurement. It is a reproducible screening metric that can reduce the number of experimental label positions before full package validation.[18] Future work should combine this static-equivalent placement result with instrumented drop tests, real printed sensor labels, adhesive-layer characterization, and package-product interaction analysis.

Acknowledgements

This work was supported by the National Research Foundation of Korea (NRF) grant funded by the Government of Korea (NRF-RS-2024-00336593).

References

1. Yam, K.L. 2009. The Wiley Encyclopedia of Packaging Technology. 3rd Ed. John Wiley & Sons, Hoboken, USA.
2. Soroka, W. 2014. Fundamentals of Packaging Technology. 5th Ed. Institute of Packaging Professionals, Naperville, USA.
3. Twede, D. and Selke, S.E.M. 2005. Cartons, Crates and Corrugated Board: Handbook of Paper and Wood Packaging

Technology. DEStech Publications, Lancaster, USA.
4. Hanlon, J.F., Kelsey, R.J. and Forcinio, H. 1998. Handbook of Package Engineering. 3rd Ed. CRC Press, Boca Raton, USA.
5. Singh, S.P., Singh, J. and Saha, K. 2015. Packaging and distribution environment considerations for e-commerce shipping. Packag. Technol. Sci. 28(8): 731-741.
6. Pawar, O.Y., Li, H., Patil, O.A., Xu, J., Dongale, T.D., Lu, B. and Lim, S. 2025. Structural transformation of graphitic carbon nitride from 2D to 1D architectures for enhanced piezoelectric performance. Chem. Eng. J. 519: 165069.
7. Priya, S. and Inman, D.J. 2009. Energy Harvesting Technologies. Springer, New York, USA.
8. Wang, Z.L. and Song, J. 2006. Piezoelectric nanogenerators based on zinc oxide nanowire arrays. Science 312(5771): 242-246.
9. Nalwa, H.S. 1995. Ferroelectric Polymers: Chemistry, Physics, and Applications. Marcel Dekker, New York, USA.
10. Lovinger, A.J. 1983. Ferroelectric polymers. Science 220 (4602): 1115-1121.
11. Martins, P., Lopes, A.C. and Lanceros-Mendez, S. 2014. Electroactive phases of poly(vinylidene fluoride): determination, processing and applications. Prog. Polym. Sci. 39(4): 683-706.
12. Wu, Z., Ding, X., Chen, X., Chen, J., Chang, X., Liu, Z., Song, L., Huang, J. and Zhu, Y. 2025. Recent progress of polymer-based piezoelectric nanogenerators. Adv. Compos. Hybrid Mater. 8: 225.
13. Ramadan, K.S., Sameoto, D. and Evoy, S. 2014. A review of piezoelectric polymers as functional materials for electromechanical transducers. Smart Mater. Struct. 23(3): 033001.
14. Aboura, Z., Talbi, N., Allaoui, S. and Benzeggagh, M.L. 2004. Elastic behavior of corrugated cardboard: experiments and modeling. Compos. Struct. 63(1): 53-62.
15. Biancolini, M.E. and Brutti, C. 2003. Numerical and experimental investigation of the strength of corrugated board packages. Packag. Technol. Sci. 16(2): 47-60.
16. Fitas, R., Schaffrath, H.J. and Schabel, S. 2025. On the design of corrugated boards: a new FEM modeling and experimental validation. arXiv:2507.02189.
17. FEFCO. 2024. What is corrugated? European Federation of Corrugated Board Manufacturers, Brussels, Belgium.
18. COMSOL AB. 2024. Structural Mechanics Module User's Guide. COMSOL AB, Stockholm, Sweden.
19. ASTM International. 2019. ASTM D4169-16: Standard Practice for Performance Testing of Shipping Containers and Systems. ASTM International, West Conshohocken, USA.
20. Stronge, W.J. 2000. Impact Mechanics. Cambridge University Press, Cambridge, UK.

투고: 2026.06.19 / 심사완료: 2026.07.06 / 게재확정: 2026.07.09